

NEUTRON SCATTERING-INDUCED BACKGROUND ENHANCEMENT IN PROMPT γ -RAY ACTIVATION ANALYSIS

D. L. ANDERSON,* E. A. MACKEY**

**Food and Drug Administration, 200 C Street SW, Washington, DC 20204 (USA)*

***University of Maryland, College Park, MD, 20742 (USA)*

(Received September 22, 1992)

Background enhancements in neutron capture prompt γ -ray activation analysis were determined over a large range of total scattering cross sections by irradiating graphite, S, Be, paraffin, urea and H₂O targets. Relative to irradiations using no target, B, Na, Cl, Al, and Pb backgrounds were 7-12 times greater with 2 ml of H₂O, but N and Fe backgrounds were only 1.2 and 1.75 times greater, respectively. For biological targets, background count rates can be determined as functions of the 2223 keV H photopeak count rate.

Introduction

Elastic neutron scattering within the target matrix has been theoretically and experimentally shown to significantly affect neutron absorption reaction rates, and therefore measured activities, for target materials in thermal neutron capture prompt γ -ray activation analysis (PGAA)¹⁻⁴. Since the scattering power of target materials varies significantly, background count rates were expected to vary as well. Background count rates for H and B have been shown to increase when targets of increasing scattering power are irradiated^{2,5}. Background γ -rays arise from neutron capture reactions with, *e.g.*, the shielding materials (H, B, C, and Pb), the detection system (N in the liquid nitrogen Dewar, and Na and I in the anti-Compton shield), the system support structure (Al, Cl, and Fe), and air (N and Ar). Since these background count rates should depend on the neutron-scattering ability of the target, the total scattering cross section for the target is defined here as $\Sigma(n\sigma_s)_t$, where n is the number of nuclei and σ_s is the total scattering cross section (cm²) for each element i in the target. Values used for σ_s are

*Present address: Inorganic Analytical Research Division, National Institute of Standards and Technology, Gaithersburg, Maryland 20899, USA.

given by Sears⁶. In this study, experiments were designed to measure the degree of enhancement for the background γ -ray count rates of H, B, Na, Cl, Al, N, Fe, and Pb and to develop simple methods for accurately correcting analytical spectral data.

Experimental

Disk-shaped targets (1.27-cm diameter) of graphite (0.39-2.16 g), S (0.52-0.90 g), paraffin (0.12-0.80 g), and urea (0.18-0.88 g) were prepared using a Carver press and Perkin-Elmer die. Nondisk geometry targets were Be (1.1 and 2.7 g, multiple shot packaged as approximately rectangular shapes), one paraffin sphere (0.44 g, fabricated with a special die²), and 1.0- and 2.0-mL aliquots of 18-megohm deionized H₂O (packaged to form 2.4 x 2.4 x 0.5-cm "pillow" shapes). All targets were packaged in Teflon film and count rates for the spectra were corrected for fluence rate variations by counting a 1.27-cm dia Ti foil monitor daily. Day-to-day fluence rates normally vary by about 0.5% (the counting statistics of the monitor) or less and are nearly constant over a typical 6-week fuel cycle within a standard deviation of about 1.5%. Background count rates with and without empty Teflon bags were determined. Irradiated materials covered a total scattering cross section range of 0 to about 6 cm². Irradiations, usually of 3 to 16-h duration, were performed at the 20 megawatt research reactor at the National Institute of Standards and Technology (NIST) in Gaithersburg, Maryland (USA), using the NIST/University of Maryland PGAA facility. The 2.5-cm dia thermal neutron beam had a fluence rate of $3.3 \times 10^8 \text{ cm}^{-2}\cdot\text{s}^{-1}$ and the detection system consisted of a 27% efficient (relative to NaI) Ge detector surrounded by a 30 x 35-cm NaI(Tl) anti-Compton shield. Findings presented here were obtained for two consecutive fuel cycles with different shielding arrangements. The H₂O targets were irradiated in the second cycle only, while some or all of the targets of other matrix types were irradiated in both cycles. Since the PGAA apparatus must be disassembled and reassembled between each fuel cycle, backgrounds differ somewhat from one cycle to the next because of positioning differences. Detailed descriptions of the methods of monitoring, the detection system, analyzer, peak fitting codes, and neutron fluence rate are described elsewhere⁵. In addition to the automatic system dead time correction, photopeak count rates were corrected for pulse pileup and neutron self-absorption⁷. The latter correction is an approximation only, as the exact relationships between neutron absorption by the target and background count rates

have not been established. However, the maximum correction for target self-absorption was only 1.3% for the 0.80-g paraffin disk, and the corrections did not significantly affect any of the findings.

Results

Al and Pb background count rates measured during the first reactor cycle are shown in Figure 1. Similar trends were found for Na and Cl. Background count rates for H were measured only for the nonhydrogenous targets of graphite, S, and Be. The 2.7-g Be target had the largest total scattering cross section of $\Sigma(n\sigma_s)_{Be} = 1.4 \text{ cm}^2$. In a separate measurement at the NIST cold neutron PGAA facility, graphite used for this experiment was shown to have an upper limit of about 50 $\mu\text{g H/g}$, which corresponds to a thermal PGAA count rate of approximately 10% of that observed for graphite in this study. Count rates produced by the Be targets and paraffin sphere were inconsistent with those produced by the disks. When only the disk-shaped target data were used, the curves for H, Na, Cl, Al, and Pb could each be fit by second-degree polynomial functions, all with correlation coefficients (R) greater than 0.98. For B (Figure 2), the graphite, Be, and urea (batch 1 only) target materials apparently contained trace, but significant amounts of B. Paraffin and a second batch of urea appeared to be "clean" with

Table 1
 $\Sigma(n\sigma_s)_t$ and H and background count rates (CPS) obtained with paraffin targets (fuel cycle 1)

$\Sigma(n\sigma_s)_t$:	0.026	0.92	3.45	6.04
H CPS:	1.721 ± 0.003	29.15 ± 0.02	108.7 ± 0.1	181.8 ± 0.1
Element (keV)	Teflon bag	120 mg	457 mg	802 mg
B (477)	0.23 ± 0.01	0.39 ± 0.01	0.68 ± 0.01	0.82 ± 0.06
Na (472)	0.053 ± 0.003	0.102 ± 0.005	0.163 ± 0.0011	0.189 ± 0.0021
Cl (6111)	0.0046 ± 0.0004	0.0082 ± 0.0007	0.015 ± 0.001	0.012 ± 0.002
Al (1779)	0.038 ± 0.001	0.078 ± 0.003	0.135 ± 0.009	0.144 ± 0.016
N (4509)	0.062 ± 0.001	0.064 ± 0.002	0.067 ± 0.002	0.074 ± 0.003
N (6323)	0.042 ± 0.001	0.045 ± 0.001	0.046 ± 0.002	0.048 ± 0.003
Fe (7632&7640)	0.0848 ± 0.0007	0.0883 ± 0.0013	0.113 ± 0.002	0.121 ± 0.003
Pb (7368)	0.0120 ± 0.0004	0.0252 ± 0.0008	0.0451 ± 0.0013	0.054 ± 0.002

Table 2

 $\Sigma(n\sigma_s)_1$ and H and background count rates (CPS) obtained with H₂O targets (fuel cycle 2)

$\Sigma(n\sigma_s)_1$:	0.04	5.68	11.24	
H CPS:	1.29 ± 0.01	196.3 ± 1.5	394.9 ± 3.2	Ratio
Element (keV)	Teflon bag	1.0 mL	2.0 mL	2.0 mL/bag
B (477)	0.217 ± 0.012	1.21 ± 0.04	1.70 ± 0.06	7.8
Na (472)	0.042 ± 0.003	0.216 ± 0.012	0.275 ± 0.019	6.5
Cl (6111)	0.0035 ± 0.0004	0.0254 ± 0.0012	0.0423 ± 0.0018	12.1
Al (1779)	0.035 ± 0.001	0.205 ± 0.009	0.294 ± 0.015	8.4
N (4509)	0.064 ± 0.001	0.071 ± 0.002	0.075 ± 0.002	1.17
N (6323)	0.0422 ± 0.0008	0.046 ± 0.001	0.052 ± 0.002	1.23
Fe (7632&7640)	0.0240 ± 0.0006	0.0343 ± 0.0012	0.0420 ± 0.0016	1.75
Pb (7368)	0.0040 ± 0.0003	0.0226 ± 0.0009	0.0359 ± 0.0012	9.0

respect to B. When only the paraffin findings were used, a second-degree polynomial fit, with an R of 0.998, was obtained.

The data for paraffin targets and a Teflon bag are presented in Table 1. Backgrounds for these elements measured with and without a Teflon bag in place were identical within the error shown. The count rates represent the overall range of $\Sigma(n\sigma_s)_1$ studied. Background count rates for B, Na, Cl, Al, and Pb were enhanced by factors of about 3 to 5 at $\Sigma(n\sigma_s)_1 = 6$ compared to those observed for the Teflon bag blank, while count rates for N and Fe were enhanced only by about 15 and 40%, respectively. Findings for the H₂O targets and a Teflon bag run during the following fuel cycle are shown in Table 2. Greater enhancements, factors of about 7-12 for B, Na, Cl, Al, and Pb, and factors of about 1.2 and 1.75 for N and Fe, respectively, were observed for 2-mL H₂O targets relative to the Teflon bag.

Discussion

For a given target shape (*i.e.*, cylinders), H, B, Na, Cl, Al, and Pb background count rates correlated well with $\Sigma(n\sigma_s)_1$, provided the element in question was not present in the target material. If the matrix of an analytical portion is well known, $\Sigma(n\sigma_s)_1$ can be calculated and cor-

rected using curves such as those in Figure 1. Since biological materials are about 5-11% H and $(\sigma_s)_H = 81.7$ barns, neutron scattering is due almost entirely to $\Sigma(n\sigma_s)_H$ and background count rates can instead be determined as a function of the H 2223-keV γ -ray photopeak count rate. Illustrating that there was no need to account for the scattering contributions from C, N,

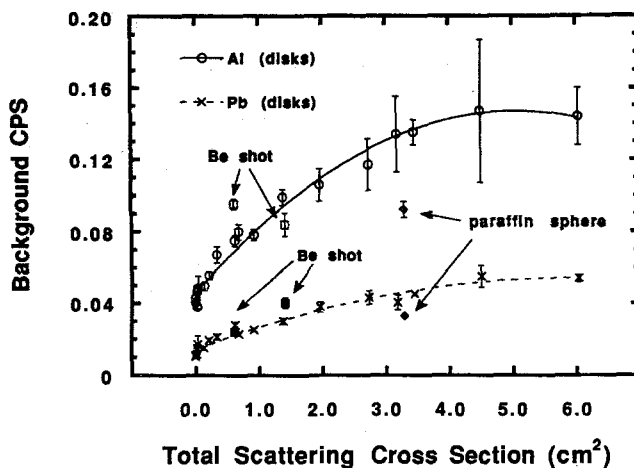


Figure 1. Background count rates in counts \cdot s $^{-1}$ (CPS) for the 1779-keV Al photopeak and the 7368-keV Pb photopeak as a function of the total scattering cross section, $\Sigma(n\sigma_s)_1$, for graphite, sulfur, urea, and paraffin disks, targetless irradiations ($\Sigma(n\sigma_s)_1 = 0$), Be shot, and a paraffin sphere. For disk-shaped targets, (Al CPS) = $0.046 + 0.0398 \cdot \Sigma(n\sigma_s)_1 - 0.00393 \cdot (\Sigma(n\sigma_s)_1)^2$, $R = 0.992$, and (Pb CPS) = $0.0144 + 0.0133 \cdot \Sigma(n\sigma_s)_1 - 0.00112 \cdot (\Sigma(n\sigma_s)_1)^2$, $R = 0.982$.

and O, regression analysis of the total H count rates vs. $\Sigma(n\sigma_s)_1$ for the disk-shaped urea and paraffin targets yielded a linear correlation with an R of 0.998. Findings such as those shown in Figure 1 indicated that the shapes and H content of the background calibration targets would have to closely approximate those of unknown analytical portions for proper background correction. For example, foods typically have H concentrations ranging from about 6 to 11%, and blanks with similar scattering characteristics (*e.g.*, similar shape and H content) must be prepared and irradiated⁷.

Since nonhydrogenous targets with total scattering cross sections similar to biological materials (about 2-6 cm² for targets of 0.75-1.0 g) could not be fabricated, background correction for H was not straightforward. The H backgrounds for disk-shaped hydrogenous matrices were estimated using the H/Al background count rate ratios obtained for the nonhydrogenous graphite and sulfur disks and the no-target and Teflon bag irradiations. Regression analysis

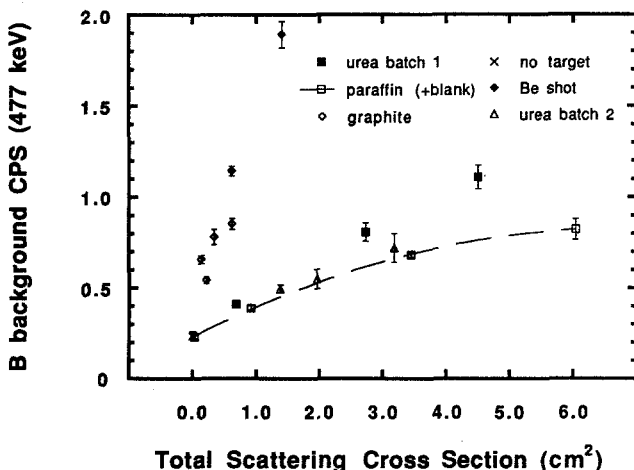


Figure 2. Background count rates in counts·s⁻¹ (CPS) for the 477-keV B photopeak as a function of the total scattering cross section, $\Sigma(n\sigma_s)_1$, for graphite, urea, and paraffin disks, targetless irradiations, and Be shot. For disk-shaped paraffin targets, $(B \text{ CPS}) = 0.229 + 0.178 \cdot \Sigma(n\sigma_s)_1 - 0.0132 \cdot (\Sigma(n\sigma_s)_1)^2$, $R = 0.9998$.

yielded an H/Al ratio of 16.9 ± 1.2 for these targets in the first reactor cycle and 32.9 ± 3.3 for the following cycle. (The beam tube and beam stop, which contain hydrogenous components, were much more heavily shielded during the second cycle.). As an approximation, this ratio was assumed to hold for hydrogenous matrices as well, and the Al (1779 keV) count rate for analytical portions was used to calculate the H background count rate for materials known to contain low Al levels. The Al concentration becomes important at levels of about 200 µg/g, which corresponds to approximately 5% of the Al background level, and using the ratio method would result in overcorrection of the H background. To avoid this problem, the H back-

ground count rate, having been calculated by H/AI ratios in the scattering blanks, was instead fit as a function of the total H count rate observed for the scattering blanks. The total H count rates of an analytical portion were then used to calculate the H background count rate for that portion, consistent with the method used for other elements. If Pb background count rates provide suitable statistics, H backgrounds may be determined in a similar fashion by using H/Pb ratios obtained from the irradiation of nonhydrogenous targets. In this study, the H/Pb background count rate was 34.9 ± 2.3 for the first reactor cycle and, because of shielding changes, 270 ± 70 for the second.

Special care must be taken to select scattering blanks that do not contain the element being characterized. In this study, for example, trace amounts of B were found in several target materials. The main source of N background (which shows only slight variation with target material) is apparently the air column through which the beam passes, since a relatively small fraction of the neutrons are scattered out of the beam. The beamstop superstructure (which is exposed to the "shadow" of the beam) and the cart supporting the anti-Compton shield are the only steel components near the detector that are exposed to the neutron field; this may explain the intermediate behavior of the Fe background count rates. Elements exhibiting strong background enhancements (with the exception of H in the beamstop) are components of materials out of the straight-through path of the beam. The hydrogenous part of the beamstop is heavily shielded, and the primary source of background for this element is probably the vertical (above floor level) beam tube and target chamber. PGAA background count rates, therefore, will also depend on the arrangement of components in an analytical facility.

*

The authors wish to thank the NIST reactor operations staff for their valuable technical assistance.

References

1. D. L. ANDERSON, W. C. CUNNINGHAM, E. A. MACKEY, *Biol. Trace Elem. Res.*, 27 (1990) 616.
2. E. A. MACKEY, Ph. D. Thesis, University of Maryland, College Park, MD, USA, 1991.
3. E. A. MACKEY, G. E. GORDON, R. M. LINDSTROM, D. L. ANDERSON, *Anal. Chem.*, 63 (1991) 288.
4. J. R. D. COPLEY, C. A. STONE, *Nucl. Instrum. Methods Phys. Res.*, A281 (1989) 593.
5. D. L. ANDERSON, W. C. CUNNINGHAM, E. A. MACKEY, *Fresen. Z. Anal. Chem.*, 338 (1990) 554.
6. V. F. SEARS, *Methods of Experimental Physics*, Vol. 23 - Part A: Neutron scattering, Academic Press, Inc., Orlando, Florida, USA, 1986.
7. D. L. ANDERSON, W. C. CUNNINGHAM, G. H. ALVAREZ, elsewhere in these proceedings.